AAS 17-271

TIME DEPENDENCE OF COLLISION PROBABILITIES DURING SATELLITE CONJUNCTIONS

Doyle T. Hall,[*] Matthew D. Hejduk,[†] and Lauren C. Johnson[‡]

The NASA Conjunction Assessment Risk Analysis (CARA) team has recently implemented updated software to calculate the probability of collision (P_c) for Earth-orbiting satellites. The algorithm can employ complex dynamical models for orbital motion, and account for the effects of non-linear trajectories as well as both position and velocity uncertainties. This "3D P_c" method entails computing a 3-dimensional numerical integral for each estimated probability. Analysis indicates that the 3D method provides several new insights over the traditional "2D P_c" method, even when approximating the orbital motion using the relatively simple Keplerian two-body dynamical model. First, the formulation provides the means to estimate variations in the time derivative of the collision probability, or the *probability rate*, R_c. For close-proximity satellites, such as those orbiting in formations or clusters, R_c variations can show multiple peaks that repeat or blend with one another, providing insight into the ongoing temporal distribution of risk. For single, isolated conjunctions, R_c analysis provides the means to identify and bound the times of peak collision risk. Additionally, analysis of multiple actual archived conjunctions demonstrates that the commonly used "2D P_c" approximation can occasionally provide inaccurate estimates. These include cases in which the 2D method yields negligibly small probabilities (*e.g.*, $P_c < 10^{-10}$), but the 3D estimates are sufficiently large to prompt increased monitoring or collision mitigation (*e.g.*, $P_c \geq 10^{-5}$). Finally, the archive analysis indicates that a relatively efficient calculation can be used to identify which conjunctions will have negligibly small probabilities. This small-P_c screening test can significantly speed the overall risk analysis computation for large numbers of conjunctions.

INTRODUCTION

As the population of artificial Earth-orbiting satellites grows, the likelihood of collisions between satellites increases. Such collisions pose a direct threat to spacecraft occupied by humans, such as the International Space Station. They also threaten a much larger number of currently active robotic satellites, which represent significant investments by many international commercial, military and scientific organizations. Collisions also pose an indirect threat to future spacecraft, through the generation of fragmentation debris that can remain orbiting for extended periods. NASA's CARA team has the responsibility to assess collision risks for a specific set of high-value satellites[1], orbiting among the much larger population of cataloged objects[#]. Much of CARA's

[*] Senior Scientist, NASA Robotic CARA, Omitron Inc., 555 E. Pikes Peak Ave, #205 Colorado Springs, CO 80903.
[†] Chief Engineer, NASA Robotic CARA, Astrorum Consulting LLC, 10006 Willow Bend Dr, Woodway, TX 76712.
[‡] Analysis Lead, NASA Robotic CARA, Omitron Inc., 555 E. Pikes Peak Ave, #205 Colorado Springs, CO 80903.
[#] See the *Space-Track* web site for more details on the cataloged satellite population: https://www.space-track.org.

effort focuses on calculating the probability of collision during conjunction events, when two satellites make a close approach to one another. Trajectories for cataloged satellites are not perfectly known; instead, they represent estimates based on tracking data gathered from a variety of sensors.[2,3] Robust P_c formulations must account for the uncertainties arising from this statistical orbital determination process.

Previous Work

Many authors have formulated analytical methods to estimate collision probabilities for Earth-orbiting satellites (see References 4-8, and references cited therein). Most of these employ some approximations that make the mathematical problem significantly more tractable, and ultimately allow P_c values to be estimated using 2-dimensional numerical integration. Specifically, these "2D P_c" methods approximate the curved relative satellite motion to be linear during the conjunction. They also assume that the duration of the conjunction is sufficiently short to allow the uncertainties on the satellite positions to be approximated as constant during the conjunction, and uncertainties on the satellite velocities to be neglected altogether. Approaches not using these approximations have also been discussed by several authors (*e.g.*, References 6-10). Specifically, in 2012, V. T. Coppola developed an approach[6] that estimates P_c values using 3-dimensional numerical integration. This "3D P_c" method – which has been adopted by the CARA team because of its comprehensive theoretical formulation – can use non-linear trajectories, and account for time-dependent uncertainties in both position and velocity.

In 2015, K. Chan noted an issue with an assumption used in the 3D P_c formulation,[11] pointing out that Coppola's integration of the flux of a time-dependent probability distribution function (PDF) through a hemi-spherical surface is not consistent with the basic tenets of probability theory. Because of this, there are limiting situations where the 3D P_c method could potentially provide inaccurate results, which can be addressed by using an alternative analytical formulation based on the *union of domains of random variables* method.[5,11] In this alternative approach, P_c values can be calculated using a 3D-volume integral within a carefully selected space of random variables. The integration volume comprises a tube swept out in this space by the collision sphere. In general this tube is curved. However, for most isolated satellite conjunctions, the tube curves gently relative to the size of the collision sphere or the PDF. In fact, the 2D P_c approximation neglects this curvature altogether. Chan's analysis[11] indicates that Coppola's method could provide inaccurate P_c estimates in three general types of conjunctions: events where this tube crosses itself, events where the tube turns too sharply, or events where the PDF expands or contracts rapidly relative to the motion of the collision sphere. Preliminary analysis of more than 80,000 archived conjunctions reveals some relatively rare occurrences (<0.5%) of the first, tube-crossing event type, and none of the latter two types. As pointed out by both Coppola[6] and Chan,[5,11] such tube crossings can potentially occur in extended encounters between close-proximity satellites which produce multiple close approach events. In these situations, P_c estimates from Coppola's method should be discarded in favor of Chan's alternative method[11] or a Monte Carlo method.[8] However, even in these situations, Coppola's probability rate R_c can still provide a useful indicator of how the collision risk varies in time. An example of such an extended encounter for two close-proximity satellites will be presented in this analysis.

Summary of the 3D P_c Implementation and Analysis

This report explains the details of CARA's recent implementation of Coppola's 3D P_c formulation, developed primarily as an incremental improvement to the current industry-standard 2D P_c estimation method. This initial 3D P_c implementation accounts for curved orbital motion as well as position and velocity uncertainties when estimating collision probabilities, and has been vali-

dated using Monte Carlo simulations of several well-studied conjunctions.[8] This report also explains how the 3D method can be used to estimate and analyze temporal variations in the collision probability rate,[12] R_c, which is equal to the time derivative of P_c for isolated conjunctions. Analysis of the probability rate provides the means to identify and bound the times of peak collision risk during isolated conjunction events much more precisely than the 2D P_c estimation method. Analysis of R_c variations also provides the means to identify times of elevated risk for extended, blended, or repeating events, which occur for satellites persistently orbiting in close proximity (*e.g.*, in clusters or formations). Such extended, blended, or repeating conjunction risks cannot be analyzed using 2D P_c methods. Finally, analysis of archived conjunctions using the 3D P_c method indicates that a relatively efficient pre-processing calculation can be used to identify which conjunctions will have negligibly small probabilities, providing the basis for a screening test that can significantly speed the risk analysis computation for large numbers of conjunctions.

OVERVIEW OF COLLISION PROBABILITY THEORY

This section provides a brief review of 2D and 3D P_c theory, focusing on how Coppola's formulation[6] can be used to estimate variations in the collision probability rate, R_c.

Satellite Orbits, Uncertainties, and Probability Density Functions

Earth-orbiting satellite trajectories are often modeled as "perturbed orbits" because the motion is affected by several perturbing forces including atmospheric drag, solar radiation pressure, solar and lunar gravity, and non-uniformities in Earth's gravitational field.[2] Satellite tracking measurements enable estimation of the parameters defining such perturbed orbits.[3] For instance, the best-estimate trajectory for a satellite "*s*" may be described by specifying its Earth-centered inertial frame (ECI) position+velocity state vector,[2] $\mathbf{x}_s(t_e) = [\mathbf{r}_s(t_e)\ \mathbf{v}_s(t_e)]$, at an initial time or epoch, t_e. Best estimate states at other times, $\mathbf{x}_s(t)$, can be propagated from this epoch state. (Note: in this discussion, such states will be considered to take the form of 6×1 column vectors.)

Uncertainties on satellite states can be described using a 6-dimensional PDF. Such PDFs can also be estimated at a particular epoch using an orbit determination analysis of multiple tracking observations, and then propagated to a time (or set of times) of interest.[3] ECI-state PDFs are often expressed using a "single-Gaussian" approximation. In this approximation, the PDF for satellite "*s*" can be written as a single multi-variate normal (MVN) function with dimensionality $d = 6$, as follows

$$\rho_s(\mathbf{y},t) \approx N_d\left(\mathbf{y},\mathbf{x}_s,\mathbf{P}_s\right) = \left[\frac{1}{\det(2\pi\mathbf{P}_s)}\right]^{1/2} \exp\left[-\frac{\left[\mathbf{y}-\mathbf{x}_s\right]^T \mathbf{P}_s^{-1}\left[\mathbf{y}-\mathbf{x}_s\right]}{2}\right] \qquad (1)$$

where $\mathbf{y}$ denotes a possible state within the distribution, $\mathbf{x}_s = \mathbf{x}_s(t)$ the center (or mean) of the distribution, $\mathbf{P}_s = \mathbf{P}_s(t)$ the 6×6 state covariance matrix, and the superscript T indicates the transpose operator. The analysis presented here employs this single-Gaussian ECI-state PDF approximation for two reasons. First, this is the same approximation generally employed when using the 2D P_c estimation method, and a large archive of actual historical conjunctions have been analyzed by the CARA team in this manner. So using this approximation in the earliest versions the 3D P_c software exploits the single-Gaussian PDF descriptions readily available from archived data, and facilitates comparison of 2D and 3D results for a long record of historical conjunctions. Second, Coppola's original formulation[6] of the basic 3D P_c equations also employs (but is not restricted to) such single-Gaussian PDFs.

While the single-Gaussian approximation in Eq. (1) has been shown to represent a reasonable approximation for high-risk ($P_c \geq 10^{-4}$) conjunctions,[13] it can be regarded as only a first step towards a more general implementation of the 3D P_c method. For instance, ECI-state PDFs can be approximated more accurately using a Gaussian mixture model (GMM)[12,14,15]

$$\rho_s(\mathbf{y},t) = \sum_{i=1}^{G_s} w_{s,i}\, N_6\left(\mathbf{y}, \mathbf{x}_{s,i}(t), \mathbf{P}_{s,i}(t)\right) \tag{2}$$

where i denotes the GMM summation index, $w_{s,i}$ the weight of the i^{th} GMM component, $\mathbf{x}_{s,i}(t)$ the center of the i^{th} component, $\mathbf{P}_{s,i}(t)$ the covariance matrix for the i^{th} component, and G_s the number of terms used in the GMM summation for satellite s. The 3D P_c formulation can be extended to use such multi-component PDFs.[6] However, this generalization comes at the cost of significant notational complexity.[12] For simplicity, the remainder of this discussion will only consider single Gaussian components. So the equations that follow can either be regarded as those appropriate for a single-Gaussian PDF approximation, or as isolated components within GMM summations (but with the associated summation indices suppressed for brevity).

Finally, the size and shape of a six dimensional MVN distribution, $N_6(\mathbf{y},\mathbf{x},\mathbf{P})$, is characterized by the 6×6 covariance matrix, $\mathbf{P}$, which can be decomposed into three 3×3 sub-matrices[6] as follows

$$\mathbf{P} = \begin{bmatrix} \mathbf{A} & \mathbf{B}^T \\ \mathbf{B} & \mathbf{C} \end{bmatrix} \tag{3}$$

These sub-matrices $\mathbf{A}$, $\mathbf{B}$ and $\mathbf{C}$ will be used later in this discussion.

Relative Satellite States and Covariances

The mean relative state for a pair of satellites (or for a pair of GMM components) can be defined as $\mathbf{x}(t) = [\mathbf{r}(t)\ \mathbf{v}(t)] = \mathbf{x}_s(t) - \mathbf{x}_p(t)$. Here, the subscripts p and s denote the primary and secondary satellites involved in a conjunction. The covariance for $\mathbf{x}(t)$ can be written $\mathbf{P}(t) = \mathbf{P}_s(t) + \mathbf{P}_p(t)$, assuming the two states $\mathbf{x}_s(t)$ and $\mathbf{x}_p(t)$ are statistically independent.[6] The relative position covariance, $\mathbf{A}(t)$, as defined in Eq. (3), can be subjected to an Eigen-decomposition to estimate the orientation and size of the uncertainty ellipsoid for the relative position vector, $\mathbf{r}(t)$, of the two satellites.[5]

Close Approach Events and Conjunctions

Most conjunctions represent single, isolated close approach events between two satellites. These occur when the magnitude of the relative position vector, $|\mathbf{r}(t)|$, reaches a minimum in time. The U.S. Air Force maintains orbital states for a large catalog of trackable satellites, enabling predictions of such close approaches for CARA's set of high-value primary satellites.[1] Conjunction analysis occurs when any cataloged secondary satellite is predicted to make an incursion into a predefined screening volume centered on a primary.[1,16] For each conjunction, the CARA system processes an *Orbital Conjunction Message* (OCM) containing many quantities, including the time of close approach (t_{ca} or TCA). The OCM also contains data that can be readily converted to the ECI states for both the primary and secondary, $\mathbf{x}_p(t_{\text{ca}})$ and $\mathbf{x}_s(t_{\text{ca}})$, respectively. These can be used to define the relative state at close approach, $\mathbf{x}(t_{\text{ca}}) = \mathbf{x}_s(t_{\text{ca}}) - \mathbf{x}_p(t_{\text{ca}})$. Other OCM data can be readily converted to the ECI-state covariance matrices for the primary and secondary, $\mathbf{P}_p(t_{\text{ca}})$ and $\mathbf{P}_s(t_{\text{ca}})$, respectively. Notably, the OCM does not contain the additional parameters required to describe the primary and secondary ECI PDFs as a multi-component GMM sum, as in Eq. (2). So using information from the OCM alone only readily enables the relative state PDF to be approximated using a single-Gaussian distribution, with ECI covariance $\mathbf{P}(t_{\text{ca}}) = \mathbf{P}_s(t_{\text{ca}}) + \mathbf{P}_p(t_{\text{ca}})$.

Approximations Used for 2D P_c Estimation

As mentioned previously, 2D P_c estimation methods use some simplifying assumptions to approximate P_c.[5,6] First, the curved relative orbital motion is approximated to be linear as follows

$$\mathbf{r}(t) \approx \mathbf{r}(t_{\text{ca}}) + \left[t - t_{\text{ca}}\right]\mathbf{v}(t_{\text{ca}}) \tag{4}$$

$$\mathbf{v}(t) \approx \mathbf{v}(t_{\text{ca}}) = \text{constant} \tag{5}$$

The 2D methods also assume that the duration of each conjunction is sufficiently short to allow two additional approximations: that the covariance of the relative position vector can be held constant during the conjunction, and that the uncertainties on the relative velocities can be neglected altogether, or

$$\mathbf{P}(t) \approx \begin{bmatrix} \mathbf{A}(t_{\text{ca}}) & \mathbf{0}_{3\times3} \\ \mathbf{0}_{3\times3} & \mathbf{0}_{3\times3} \end{bmatrix} = \text{constant} \tag{6}$$

where $\mathbf{0}_{3\times3}$ denotes a 3×3 matrix of zeros.[6] Using these approximations, the 2D methods can efficiently estimate a single P_c value for each conjunction.[4,5]

Some conjunctions violate the assumptions behind these 2D P_c approximations.[7,8] For instance, not all conjunctions have a sufficiently short duration to justify their use. As discussed below, formulations to estimate conjunction durations[5,7] can be used to show that some events have extremely long durations, comparable to the orbital periods of the primary or secondary satellites. Also, for satellite pairs persistently orbiting in close proximity, the concept of a single, isolated conjunction can break down altogether, because the events can repeat in a nearly periodic fashion, and become so extended that they blend into one another.

Conjunction Bounds, Midpoints, and Durations

This analysis estimates conjunction durations using a method also developed by Coppola.[7] Although this formulation strictly applies to conjunctions analyzed using the 2D P_c method, analysis indicates that it serves as a useful first-cut approximation for 3D conjunctions as well. The formulation[7] denotes the beginning and ending bounding times of a conjunction as $\tau_0(\gamma)$ and $\tau_1(\gamma)$, respectively, where γ is a small number that defines a measure of achievable numerical precision, taken here to be $\gamma = 10^{-16}$, roughly the resolution limit for computed double precision values. The conjunction duration spans these bounds: $\Delta\tau = \tau_1 - \tau_0$. Similarly, the conjunction midpoint is defined here to bisect these bounds: $\tau_m = (\tau_1 + \tau_0)/2$.

Other formulations to estimate conjunction durations[5] have been demonstrated to be consistent with the method[7] employed here. However, it should be reemphasized that these methods only strictly apply when using the short-encounter assumptions of the 2D P_c method[7] – *i.e.*, the linearized dynamical model given in Eqs. (4)–(6). As will be discussed in more detail later, these conjunction durations and bounds do not always bracket the times of peak collision risk that occur when calculating 3D P_c values using more advanced dynamical models. In these cases, these first-cut conjunction bounds must be expanded appropriately.

Formulation for 3D P_c Estimation

The 3D P_c formulation (also referred to as the *direct* method[12]) does not employ the restrictive 2D-method assumptions discussed above, but instead can use relative ECI states and covariances from a dynamical model to estimate collision probabilities.[6] This dynamical model must provide

the following set of time-dependent quantities: {**x**(*t*), **P**(*t*)}, or alternatively {**x**(*t*), **A**(*t*), **B**(*t*), **C**(*t*)}. During the calculation, these quantities can be propagated from a reference epoch, or interpolated from a pre-tabulated ephemeris. The dynamical model could, conceivably, be very complex by including the effects of many perturbative forces. This approach would yield accurate results, but at the cost of considerable computation, some of which may not be required to achieve sufficient accuracy. Alternatively, the dynamical model could be very simple. For instance, nothing should prevent properly implemented 3D P_c software from using the linearized dynamical model given in Eqs. (4)–(6). In this case, the 3D computation should always closely reproduce 2D P_c values, as will be shown later.

To demonstrate some of the differences that can arise between the 2D and 3D methods, this analysis also employs a slightly more complex dynamical model: Keplerian two-body orbital motion[2] which describes elliptical trajectories within a uniform $1/r^2$ gravitational field of a central body. This dynamical model still represents an approximation, because it neglects the effects of many important perturbative forces. However, over sufficiently short time intervals it does approximate the curved shape of the trajectories, and allows the full 6×6 covariances to be propagated in time.[17]

The expression for the 3D collision probability can be written as the sum of two components,[6] $P_c = P_0 + P_I$. Here, P_0 indicates the probability at an initial time, t_0, and can often be neglected unless t_0 lies too close to a moment of peak collision risk. P_I indicates the subsequent cumulative probability integrated over a finite time interval, $t_0 < t \le t_0 + T$. The CARA software explicitly calculates and includes P_0 when estimating 3D P_c values. However, for simplicity, the remainder of this discussion will suppress P_0, which allows the symbols P_c and P_I to be used interchangeably. With this simplification, P_c could be expressed using a single equation containing a three-dimensional integral, as in Eq. (38b) of the original Coppola formulation.[6] However, following the formulation of DeMars *et al* [12], this analysis separates the expression into two equations in order to provide more insight into the time dependence of collision risk. The first equation contains the outermost integral over time

$$P_c = \int_{t_0}^{t_0+T} R_c(t)\,dt \tag{7}$$

The second equation for the time-dependent probability rate,[12] $R_c(t)$, contains the innermost two-dimensional integral, which spans the unit sphere

$$R_c(t) = \frac{dP_c}{dt} = \oint_{4\pi} I(\hat{\mathbf{r}}, t)\, d^2\hat{\mathbf{r}} \tag{8}$$

The integrand for this equation, denoted here using the symbol I, maps between points on the unit sphere and time, but also depends on the dynamical model quantities {**x**(*t*), **P**(*t*)}. This integrand comprises three factors, one of which is the square of the combined primary+secondary hard-body radii. The other two factors of I require several equations to describe fully.[6,12] These details are not repeated here. Instead, this discussion focuses on gaining a better understanding of the time dependence of collision risk provided by isolating the expression for the probability rate $R_c(t)$, and analyzing the associated temporal variations. For instance, as will be shown below, an isolated conjunction generally produces an $R_c(t)$ function with a single peak in time, which represents the moment of greatest collision risk. Satellites orbiting in close proximity, on the other hand, can produce multiple R_c peaks.

Monte Carlo P_c Estimation

Collision probabilities can also be estimated using Monte Carlo simulation methods.[8,12] These can be computationally intensive because they require repeatedly performing the following algorithmic steps: 1) sample the state PDFs of the primary and secondary satellites at some time; 2) propagate the sampled states over the conjunction time interval of interest, explicitly checking if the intervening distance ever becomes less than the combined hard-body radii; and 3) if so, register that a collision has occurred at the time of first contact between the two spheres defined by those radii. These steps need to be repeated until enough simulated collisions have been registered to provide sufficiently accurate statistical results. Step 2 requires the most computation, especially for complex dynamical models. However, for the linearized model in Eqs. (4) and (5), this step can be performed analytically, meaning that such simulations can be performed relatively quickly.

In the sections below, calculations using the 3D method of Eqs. (7) and (8) will be compared to Monte Carlo simulations using both the linearized dynamical model and the more computationally intensive Keplerian two-body model. For these comparisons, the sampling performed in Monte Carlo step 1 above employs the single-Gaussian ECI-state distributions readily provided by the archived OCMs, as discussed above. Comparisons using more complex PDFs (*e.g.*, multi-component GMMs) and/or more advanced dynamical models (*e.g.*, high-fidelity state+covariance propagators) will be deferred for future analyses.

CARA IMPLEMENTATION OF 3D P_C ESTIMATION

This section outlines the details of how CARA's 3D P_c software calculates the integrals in Eqs. (7) and (8) numerically, as well as how the Keplerian two-body dynamical model has been implemented as a first step towards a more general and accurate approach.

Numerical Integration over Time

The 1D integral over time in Eq. (7) can be calculated using numerical techniques such as Simpson's rule integration[6] or trapezoidal integration. Both of these schemes require that the integration limits and step sizes be adjusted to achieve a desired numerical accuracy. As mentioned previously, the conjunction bounds (τ_0, τ_1) only provide a first-cut approximation for the integration limits when using the Keplerian two-body dynamical model. For instance, the archive study indicates that, even for isolated conjunctions, (τ_0, τ_1) do not always necessarily bracket the time when $R_c(t)$ peaks. Also, for archived conjunctions involving close-proximity satellites, (τ_0, τ_1) can fail to bracket one or more of the repeating peaks in $R_c(t)$. Ideally, these first-cut integration limits should be adjusted as required during the computation to account for these effects, dynamically refined in order to find and sufficiently bracket all of the numerically significant peaks in $R_c(t)$. Similarly, the integration step size should also be dynamically adjusted. The CARA team plans to implement such adaptive integration schemes in future versions of the software. Currently, however, the conjunction bounds are simply expanded by a user-specified factor, E, resulting in the following lower and upper integration limits

$$t_0 = \tau_m - E\left(\frac{\Delta\tau}{2}\right) \tag{9}$$

$$t_0 + T = \tau_m + E\left(\frac{\Delta\tau}{2}\right) \tag{10}$$

where $\Delta\tau$ and τ_m denote the conjunction duration and midpoint defined previously. When using the linearized dynamical model from Eqs. (4)–(6), an expansion factor of $E = 1$ should always suffice for these integration limits.[7] Preliminary analysis indicates that for the Keplerian two-body dynamical model, E factors of 2 to 5, along with an integration step size of $h \approx \Delta\tau/100$, often suffice for single, isolated conjunctions. More conservatively, the expansion can be increased to $E = 10$, but often at the cost of more computation with no significant increase in integration accuracy. However, this simplified expansion approach does not address cases where there are multiple peaks in $R_c(t)$, where, as mentioned previously, the concept of a single conjunction with well-defined temporal limits can break down altogether. Also, some cases have been found where the integration step size of $h \approx \Delta\tau/100$ seems to be too coarse, causing Simpson's rule integrations to show unstable convergence behavior; for this reason, the current version of CARA's software uses trapezoidal integration, which is less susceptible to such instabilities.

Numerical Integration over the Unit Sphere

The 2D unit sphere integral in Eq. (8) can be evaluated efficiently using a scheme called Lebedev quadrature.[6,12,18] This method computes the 2D integral using a single weighted summation over a set of pre-defined points on the unit sphere. Quadrature points and weights have been defined[18] for many different spherical harmonic or algebraic orders, up to a maximum of 131. Increasing the algebraic order provides better integration accuracy at the cost of increased computation. The CARA team plans eventually to implement a dynamic, self-adjusting integration scheme for this unit sphere integration. However, the current version of CARA's software simply uses the maximum available Lebedev algebraic order of 131, which entails a weighted sum over 5810 points.

Covariance Propagation for Keplerian Two-Body Motion

When using the Keplerian two-body dynamical model, CARA's 3D P_c software currently propagates ECI-frame covariances using analytically-derived state transition matrices.[17] More specifically, the software employs the equation $\mathbf{P}(t) = \mathbf{\Phi}\,\mathbf{P}(t_{ca})\,\mathbf{\Phi}^T$, where $\mathbf{\Phi} = \mathbf{\Phi}(t, t_{ca})$ indicates the state-deviation transition matrix for two-body motion published by Shepperd.[17] This method of covariance propagation could be improved, because it can fail to produce realistic estimates for $\mathbf{P}(t)$ over long propagation periods.[12,19,20] For instance, propagating covariances expressed in equinoctial orbital elements may be a better approach[19] especially for more complex dynamical models.[20] However, one of the goals of the current analysis is to compare the 2D and 3D P_c methods, and investigate differences that can potentially arise by introducing nonlinear motion and time-dependent 6×6 covariances. This goal can be accomplished using Shepperd's state transition matrix formulation. However, once again, the CARA team regards this as only a first step towards a more general and robust approach.

VALIDATION USING WELL-STUDIED CONJUNCTIONS

In 2009, Alfano published a discussion of twelve conjunctions analyzed in detail using Monte Carlo and other P_c estimation methods.[8] This includes one case where the 2D and Monte Carlo P_c methods match one another very well, but also several cases where the 2D P_c method fails to reproduce the Monte Carlo calculations. These well-studied conjunctions provide the means to validate the implementation of CARA's new 3D P_c software. Specifically, Alfano's Monte Carlo analyses for these cases provide benchmark P_c values that should be closely reproduced by the 3D P_c software, if properly implemented. The discussion below focuses on two of these benchmark cases, selected to illustrate that the newly-implemented 3D P_c software does indeed reproduce Alfano's results (as it also does for the other benchmark cases not discussed or shown here).

Validation Using Alfano's Test Case 3

Figure 1 shows the results of an analysis of "linear" test case 3, demonstrated by Alfano to be a conjunction where the 2D and Monte Carlo P_c methods match one another.[8] The left panel plots the probability rate as a function of time, and the right panel plots the associated cumulative probability. Legends above each panel describe the plotted quantities and calculated P_c values. The black points in each panel show the results of CARA's Monte Carlo simulation using the linearized dynamical model from Eqs. (4)–(6), with a sample size of 30 million. The green curves show the output from CARA's 3D P_c software, also using the linearized dynamical model and an expansion factor of $E = 1$. The vertical cyan lines in the left panel show the conjunction bounds (τ_0, τ_1), which bracket the peak in probability rate (and which serve as the temporal integration limits in this case because $E = 1$). The horizontal magenta line in the right panel shows the calculated 2D P_c value (labeled in the legend as "Foster P_c", in reference to the first author of an early formulation of the 2D method[4]). As discussed previously, when the 3D P_c software is driven using these linearized inputs, it should always closely reproduce the 2D P_c value; the convergence of the green curve and the magenta line in the right panel demonstrates this explicitly. For this case, Alfano's Monte Carlo simulation using 30 million samples yields $P_c = 0.10034$, essentially identical to CARA's 3D and Monte Carlo P_c estimates cited in the figure legend.

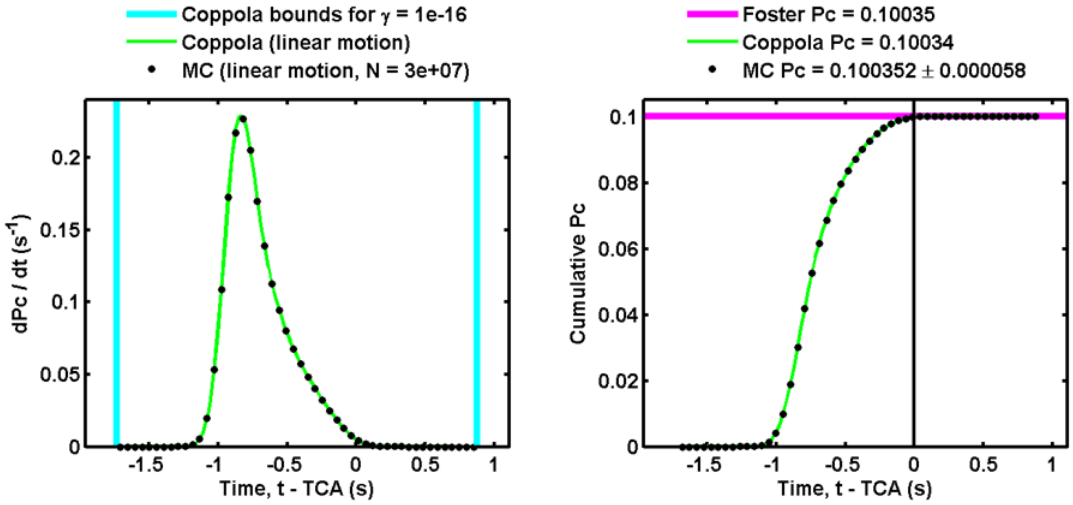

Figure 1. Linearized-mode validation plots for Alfano's conjunction test case 3.

Step-by-Step Relaxation of the 2D P_c Assumptions

The assumptions employed in the 2D P_c approximation can be relaxed in a step-by-step fashion, which provides additional insight when validating cases for which the 2D and 3D methods disagree. For the first step, the 3D P_c software uses the linearized dynamical model from Eqs. (4)–(6), where it should always reproduce the 2D P_c values, as demonstrated in the previous section. This first step can be described succinctly using the identifier "Linear motion, **A**=**A**(TCA), **B**=**C**=**0**," notation which will appear on the legends of several figures presented later. For the second relaxation step, the linear motion can be replaced with Keplerian two-body motion, but the approximations of Eq. (6) left intact, described succinctly as "Kep2Body, **A**=**A**(TCA), **B**=**C**=**0**." The third step introduces the time dependence of the relative position covariance, or "Kep2Body, **A**=**A**(*t*), **B**=**C**=**0**." Finally, the fourth step introduces the full 6×6 time-dependent covariance matrix, or "Kep2Body, **P** = **P**(*t*)." These relaxation steps define four operating modes of CARA's current 3D P_c software, identified

here as "Coppola 1" through "Coppola 4," respectively. Among these, the fourth mode "Coppola 4" provides the current best estimate 3D P_c values, to be compared to Alfano's Monte Carlo benchmark P_c values for this validation study.

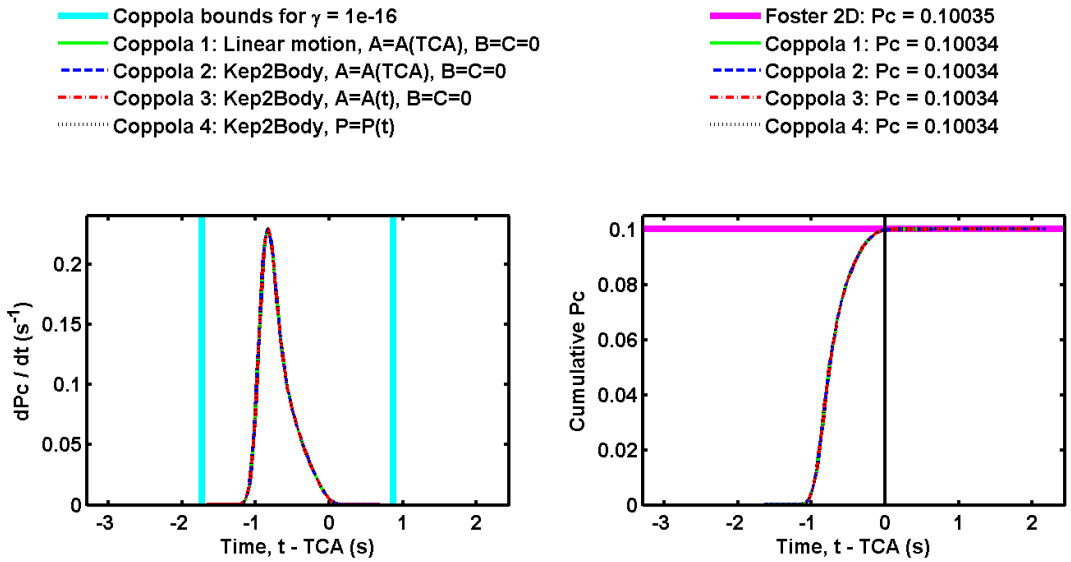

Figure 2. Step-by-step relaxation plots for Alfano's conjunction test case 3.

Figure 2 shows such a step-by-step relaxation analysis for Alfano's linear test case 3, the same case shown in Figure 1. Again the two panels plot R_c (left) and cumulative P_c (right) against time. Curves for all four relaxation steps represent output from the 3D P_c software, with the first step using an expansion factor of $E = 1$ and the other three $E = 2$. Legends above each panel show the plotted quantities and calculated P_c values. The curves for all four of these relaxation steps plot directly on top of one another, and match the Foster 2D result, as they should for this benchmark case where the 2D and 3D methods are known to agree.[8]

Validation Using Alfano's Test Case 10

Figure 3 shows a step-by-step relaxation analysis of Alfano's "nonlinear" test case 10, using the same format as Figure 2. Again, curves for all four steps represent output from the 3D P_c software, with the first step using an expansion factor of $E = 1$, but the other three requiring $E \approx 5$ for satisfactory integration convergence for this long duration conjunction. These plots clearly show that the four relaxation steps each produce distinctly different results. This is not surprising, because Alfano's analysis[8] demonstrates that for this case the 2D and Monte Carlo P_c values disagree, indicating that one or more of the assumptions used in the 2D method has been violated. Alfano's Monte Carlo simulation using 1 billion samples yields a benchmark $P_c = 0.36300$, differing by only 0.3% from the best estimate 3D P_c value of 0.36406. Both of these results differ significantly from the 2D estimate of $P_c = 0.29016$.

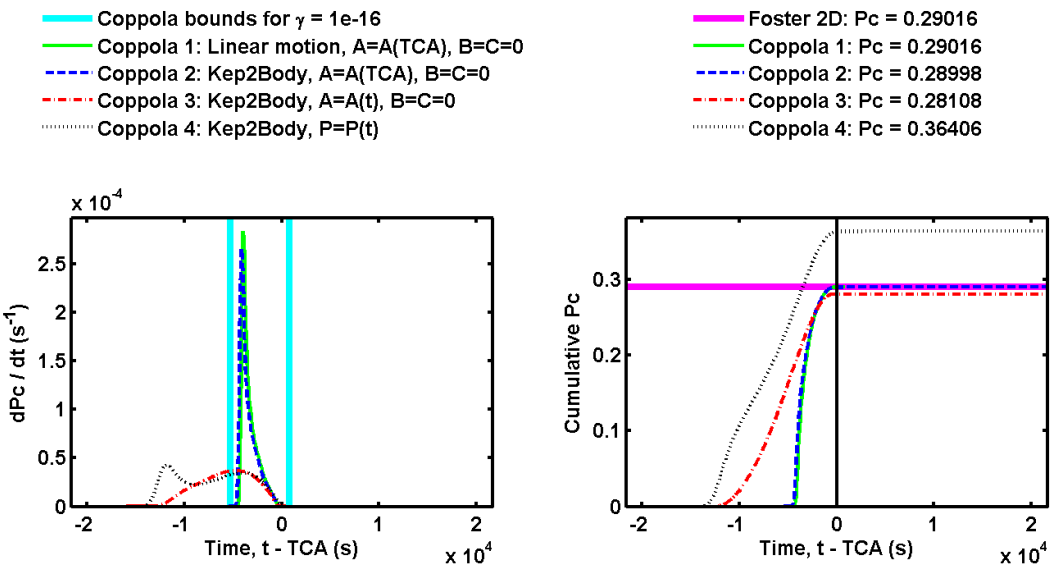

Figure 3. Step-by-step relaxation plots for Alfano's conjunction test case 10.

Figure 4 shows this same test case 10 analyzed using CARA's Monte Carlo simulation software with 3 million samples (orange diamonds) compared to the best estimate results from the 3D P_c software (dotted black curve). In this case, the temporal integration limits have been adjusted to match those used in Alfano's original analysis.[8] Clearly, CARA's Monte Carlo simulation closely reproduces the 3D P_c software results, and both match Alfano's benchmark P_c value to within 0.3%. The left panel of Figure 4 clearly indicates that this long duration conjunction comprises two $R_c(t)$ peaks which occur sufficiently close in time that they blend together. Inspection of the cumulative P_c plotted as the dotted black curve in the right panel indicates that the 3D P_c calculation reproduces Alfano's corresponding benchmark curve (see Figure A10 of Reference 8).

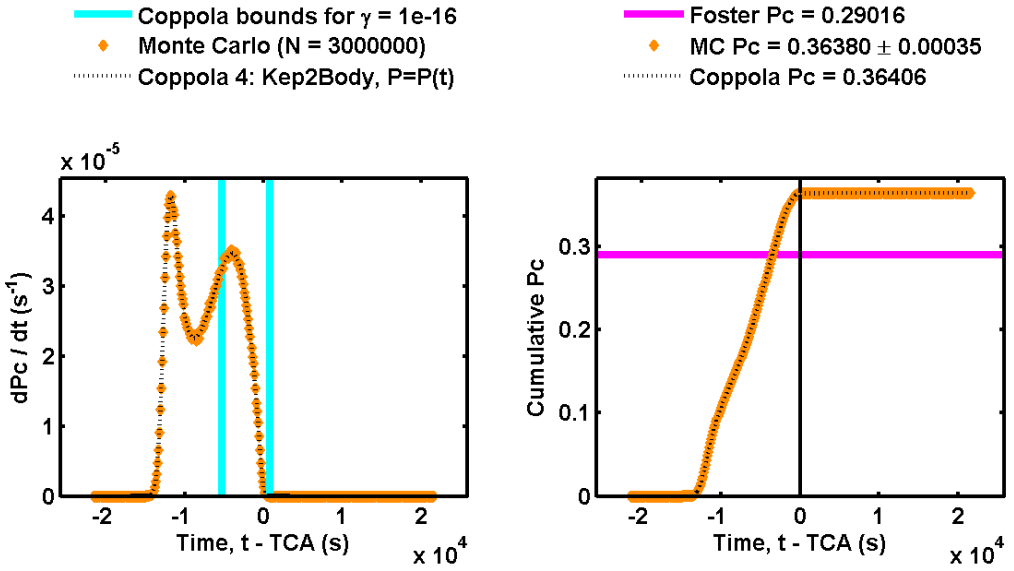

Figure 4. Monte Carlo and 3D method analysis for Alfano's conjunction test case 10.

ANALYSIS OF ARCHIVED CONJUNCTION EVENTS

This section describes the preliminary analysis of some actual historical conjunctions previously analyzed by the CARA team. Specifically, the analysis employs a set of 80,827 archived OCMs, representing conjunctions that occurred between 2016-04-01 and 2016-06-19. Of these, 80,453 are evaluated to be "high quality" events, characterized by positive-definite covariances $\mathbf{A}(t_{ca})$ and $\mathbf{P}(t_{ca})$.

Extended, Blended or Repeating Conjunction Events

Satellites persistently orbiting in close proximity (*e.g.*, formation flying) can make repeated close approaches to one another and produce a probability rate curve $R_c(t)$ with multiple blended peaks. Figure 55 shows $R_c(t)$ curves calculated from an archived OCM involving two close-proximity satellites. The solid green curve uses all of the 2D P_c assumptions and produces a single isolated $R_c(t)$ peak, as it should. However, the dashed blue curve shows that introducing Keplerian two-body motion leads to multiple peaks, caused by repeated encounters between the two satellites. Introducing propagated covariances can then change the shape of these peaks. The $R_c(t)$ curve estimated using the full Keplerian two-body dynamical model, plotted as the dotted black curve, clearly shows multiple, repeating peaks that blend together. Notably, the repeating, nearly periodic nature of this probability rate curve is likely an artifact of the relatively simple two-body motion model employed here; the effect of orbital perturbations included in more advanced dynamical models would likely create more pronounced differences between the sequential peaks.

Extended, repeating or blended events can be identified by analyzing conjunction durations. For instance, all such events contained in this archive analysis can be identified as those with a conjunction duration, $\Delta\tau$, larger than ≈1% of the minimum orbital period for the two objects, T_{min}. For example, $\Delta\tau/T_{min}$ equals 14% and 65% for the cases shown in Figures 4 and 555, respectively. Of the original 80,453 high quality archived conjunctions, 346 have $\Delta\tau/T_{min} \geq 1\%$, and produce repeating probability rate curves qualitatively similar to that plotted in Figure 55. The remaining 80,107 OCMs represent single-peaked conjunctions (referred to in this analysis as "isolated" conjunctions).

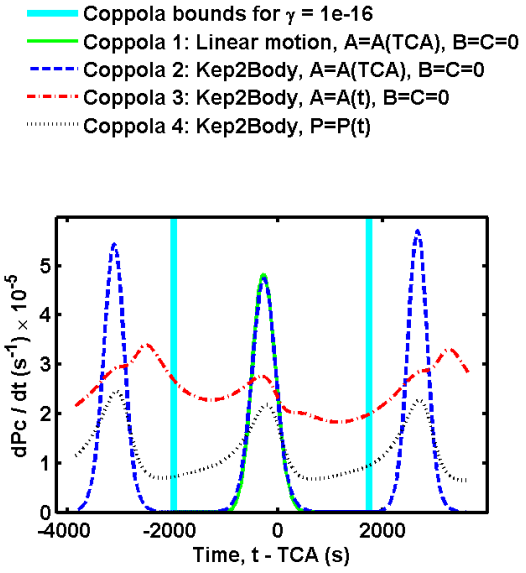

Figure 5. A plot of the probability rate for two close-proximity satellites.

As mentioned previously, such repeating encounters between close-proximity satellites can potentially cause Coppola's formulation to yield inaccurate P_c estimates.[6,11] In these cases, the CARA team uses instead P_c estimates from a Monte Carlo method, which does not suffer from this limitation. Notably, in these cases, the P_c estimates from Coppola's method (i.e., those derived by performing an integration over the dotted black curve in Figure 55) generally erroneously exceed the Monte Carlo P_c values. As pointed out by Chan,[11] these erroneously large P_c values can potentially even exceed unity, re-emphasizing the limitations of Coppola's formulation in these situations. Despite this, the multi-peaked $R_c(t)$ variations still provide a useful indicator of the times and frequencies of elevated collision risk for such close-proximity satellites, even though the R_c integral in Eq. (8) potentially no longer provides an accurate approximation for dP_c/dt.

The Frequency of 2D and 3D P_c Discrepancies

After eliminating the extended, repeating or blended conjunctions from the archived data as described above, most of the remaining 80,107 cases were found to have negligibly small 3D P_c values. For instance, the software returns a 3D P_c value numerically equal to zero for 44,970 (or 56%) of these. Only 11,211 (14%) were found to have $P_c \geq 10^{-15}$, and 8,269 (10%) with $P_c \geq 10^{-10}$. Finally, the CARA team often uses a threshold of $P_c \geq 10^{-7}$ for initiating follow-up analyses, and only 5,761 (7.2%) of the cases exceeded this threshold.

Similarly, only 2,674 (or 3.3%) were found to have 3D $P_c \geq 10^{-5}$, which represents the most important set for the CARA team. For this set, most 2D and 3D P_c estimates were found to be relatively close to one another: 1462 (55%) were found to be within 3% of one another, 1,912 (71%) within 10% of one another, and 2266 (85%) within 30%. Smaller subsets showed larger discrepancies: 216 (8.1%) were found to differ by a factor of 2 or more, 149 (5.6%) by a factor of 3 or more; and 64 (2.4%) by 10 or more. These more discrepant subsets include cases where the 2D P_c estimate is both much greater as well as much smaller than the 3D estimate, which produce *false alarms* and *misdetections*, respectively.[20] The misdetections where 3D P_c >> 2D P_c concern the CARA team most. Specifically, the existence of such cases in the archive suggests that a small fraction of historical conjunctions with significant risk may have been overlooked because of inaccurately low 2D P_c estimation. Figures 6 and 7 show plots for two such examples, where the 3D P_c value exceeds the 2D value by a factor of about four and by several orders of magnitude, respectively.

The CARA team continues to analyze the nature and frequency of such large 2D vs. 3D method discrepancies for isolated conjunctions. One notable and intriguing feature that such discrepant conjunctions seem to show is that the conjunction bounds (τ_0, τ_1) often do not bracket the time of closest approach. This is true for both of the cases plotted in Figures 6 and 7. Other features often shown by the most widely discrepant cases are that the peak in the probability rate curve can become relatively thin and/or occur relatively far from the conjunction midpoint time, both of which can be seen in Figure 7. In other discrepant cases not shown here, the (τ_0, τ_1) bounds do not even bracket the $R_c(t)$ peak. These effects reinforce the need to implement an adaptive algorithm to calculate the temporal integration limits and step-sizes used when numerically calculating the integral in Eq. (7), as discussed previously.

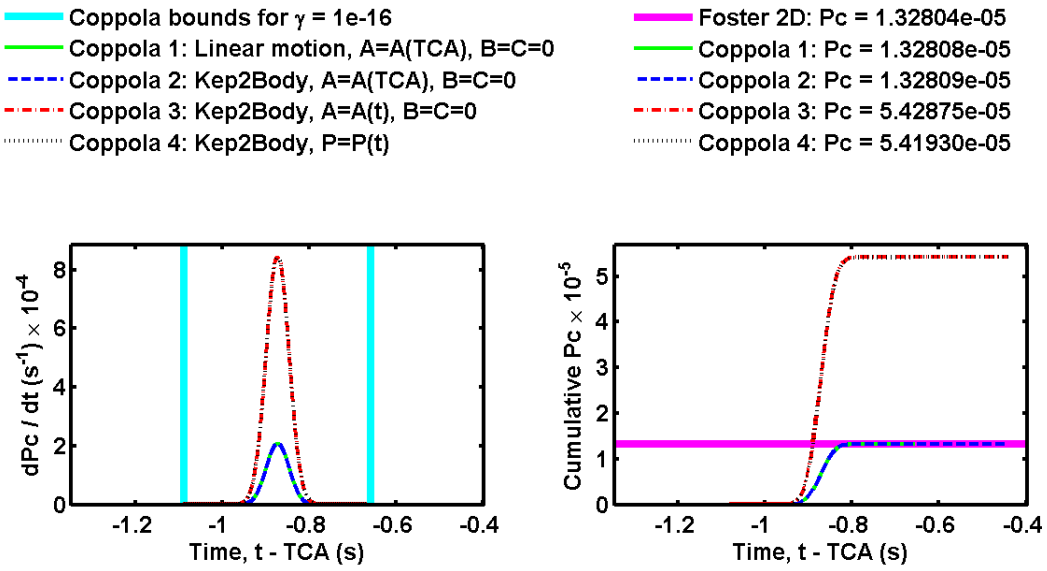

Figure 6. An archived conjunction event where the 2D and 3D Pc values differ by a factor of ≈4.

Other cases of large 2D vs. 3D discrepancies also seem to be characterized by poor quality covariance matrices. In this analysis, cases where the relative covariances $\mathbf{A}(t_{ca})$ and $\mathbf{P}(t_{ca})$ are not positive-definite have been eliminated from the analysis. However, some discrepant conjunctions that pass this test may still have one (or more) low-quality primary and/or secondary covariances among the set $\{\mathbf{A}_p(t_{ca}), \mathbf{P}_p(t_{ca}), \mathbf{A}_s(t_{ca}), \mathbf{P}_s(t_{ca})\}$. Again, the CARA team continues to analyze the nature and frequency of such discrepancies.

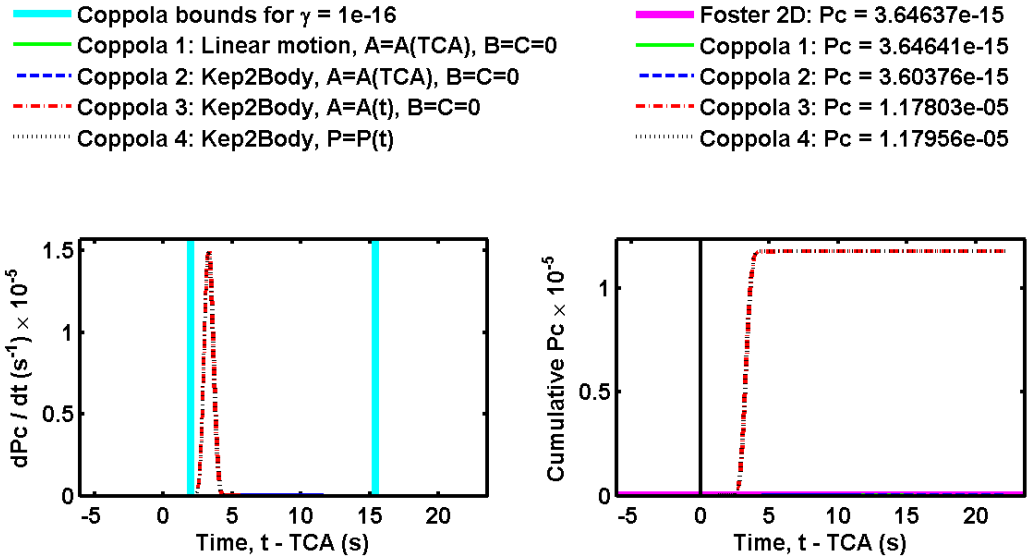

Figure 7. An archived event where the 2D and 3D Pc values differ by several orders of magnitude.

Finally, the specific discrepant cases noted so far have all occurred when using the current version of CARA's 3D P_c software *which employs the Keplerian two-body dynamical model and single-Gaussian ECI-state PDF approximations.* As stated previously, the current implementation

using these approximations only represents a first step, to be followed by a series of upgrades to create a more general and accurate implementation of the method. After such upgrades, the specific discrepant cases noted here may change or vanish, but likely to be replaced by other similarly discrepant cases (see Reference 20). However, the plots shown in this initial analysis sufficiently illustrate that, for isolated conjunctions, the time of peak collision risk does not necessarily coincide with the time of closest approach or even with the conjunction midpoint time, and that the 2D approximation can potentially produce very inaccurate results for some conjunctions.

A Small-P_c Screening Test Based on Mahalanobis Distances

The archive analysis also indicates that a relatively efficient calculation can identify which conjunctions will have negligibly small probabilities when using the single-Gaussian PDF approximation. This small-P_c screening calculation exploits a correlation found to exist between 3D P_c values and relative-state Mahalanobis distances. More specifically, the P_c value for an isolated conjunction correlates strongly with the *minimum relative position Mahalanobis distance that occurs during the event*, as explained below.

The relative position Mahalanobis distance is a time-dependent quantity defined as follows

$$M_D(t) = \left[\mathbf{r}^T \, \mathbf{A}^{-1} \, \mathbf{r}\right]^{1/2} \tag{11}$$

where the time dependence on the relative position vector **r** and relative position covariance **A** have been suppressed. During an isolated conjunction event, this Mahalanobis distance first decreases as the two satellites approach one another, reaches a minimum value, and then increases as they separate. The time and value of this minimum Mahalanobis distance can be found using numerical methods. Notably, the time that $M_D(t)$ minimizes does not generally coincide with the time of closest approach. Analysis of archived conjunctions indicates that it often coincides more closely with the conjunction midpoint time, and even more closely yet with the time that the probability rate peaks. Analysis also indicates that 3D P_c values correlate strongly with the minimum M_D value, as shown in Figure 8. The blue crosses show conjunctions with minimum $M_D \leq 10$. The red crosses show cases with minimum $M_D > 10$; this larger set comprises about 80% of the conjunctions, all of which have $P_c < 3\times10^{-17}$, a negligibly small value from the CARA team's perspective.

The strong correlation apparent in Figure 8 can be used as a basis for an efficient small-P_c screening test. Specifically, about 80% of the 3D P_c calculations can be circumvented by precomputing the minimum Mahalanobis distance for each conjunction, and eliminating those with values larger than 10. The efficiency arises because Mahalanobis distances require significantly less computation than 3D P_c values. As described previously, the analysis that produced Figure 8 employs the single-Gaussian PDF and Keplerian two-body motion approximations, but only as a first step towards more advanced approaches. These more advanced models will also likely produce a correlation like that in Figure 8, which can then be similarly exploited for small-P_c screening. Furthermore, because these more advanced models will likely require even more intensive computation to calculate 3D P_c values, performing such screening will potentially become more important when analyzing large sets of conjunctions.

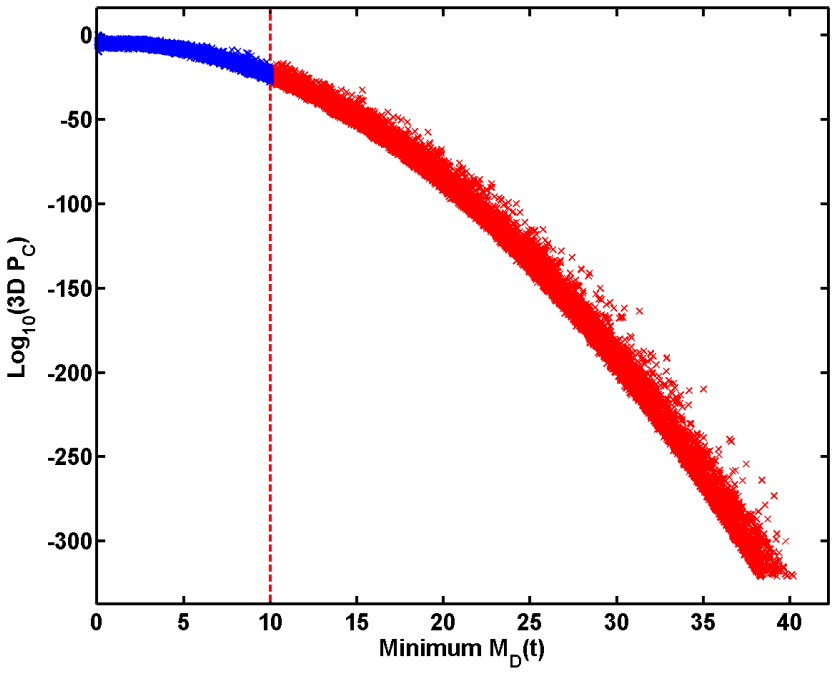

Figure 8. The correlation between 3D Pc and minimum Mahalanobis distance.

CONCLUSIONS AND FUTURE WORK

The implementation of the 3D P_c estimation method formulated by Coppola[6] provides several new insights for the conjunction risk assessment community. Many of these insights arise because the formulation provides estimates of the probability rate, $R_c(t)$. For close-proximity satellites, variations in $R_c(t)$ can show multiple peaks that repeat or blend with one another, providing a new way to view the temporal distribution of risk. For isolated conjunctions, $R_c(t)$ analysis provides the means to identify and bound times of peak collision risk, which do not always coincide with times of close approach or with conjunction midpoint times. Analysis of archived conjunction data demonstrates that the commonly used 2D P_c approximation can occasionally provide inaccurate estimates, including misdetections where the 3D P_c value exceeds the 2D value by several orders of magnitude. The 3D method also provides the basis for a small-P_c screening test that can significantly speed risk analysis computations for large numbers of conjunctions.

As mentioned previously, the CARA team has employed several approximations for the initial 3D P_c software implementation presented here. Future enhancements may entail relaxing the assumptions behind these approximations and using more advanced algorithms, including:

1. Adaptive quadrature schemes for the numerical integrations in Eqs. (7) and (8).
2. Higher fidelity dynamical models, such as state propagation that includes all relevant orbital perturbations.
3. More advanced covariance propagation such as that derived from an Equinoctial orbital element description.[19,20]
4. More realistic state PDF representations, such as the GMM expansion from Eq. (2).[12,14,15,20]

By implementing these upgrades, we believe that the 3D P_c method has the potential to provide substantially more realistic and accurate conjunction risk assessments.

ACKNOWLEDGMENTS

The authors would like to thank Salvatore Alfano for providing files containing the conjunction test case data from Reference 8, Russell Carpenter for providing an early software implementation of Coppola's P_c formulation, Joseph Frisbee for several helpful discussions and analyses, and Kenneth Chan for providing his relevant publications concerning Coppola's P_c formulation.

REFERENCES

[1] L.K. Newman and M.D. Hejduk, "NASA Conjunction Assessment Organizational Approach and the Associated Determination of Screening Volume Sizes," *International CA Risk Assessment Workshop*, 19-20 May 2015.

[2] D.A. Vallado, *Fundamentals of Astrodynamics and Applications*, 2rd ed., Microcosm Press, El Segundo CA, 2001.

[3] B.D. Tapley, B.E. Schutz, and G.H. Born, *Statistical Orbit Determination*, Elsevier Academic Press, Burlington, MA, 2004.

[4] J. L. Foster and H. S. Estes, "A Parametric Analysis of Orbital Debris Collision Probability and Maneuver Rate for Space Vehicles," NASA/JSC-25898, Aug. 1992.

[5] K. Chan, *Spacecraft Collision Probability*, El Segundo, CA, The AeroSpace Corporation, 2008.

[6] V.T. Coppola, "Including Velocity Uncertainty in the Probability of Collision between Space Objects," *AAS/AIAA Spaceflight Mechanics Meeting*, Charleston SC, Paper 12-247, Feb. 2012.

[7] V.T. Coppola, "Evaluating the Short Encounter Assumption of the Probability of Collision Formula," *AAS/AIAA Spaceflight Mechanics Meeting*, Charleston SC, Paper 12-248, Feb. 2012.

[8] S. Alfano, "Satellite Conjunction Monte Carlo Analysis," *AAS SpaceFlight Mechanics Meeting*, Pittsburgh, PA, Paper 09-233, Feb. 2009.

[9] R.P. Patera, "Satellite Collision Probability for Nonlinear Relative Motion," *Journal of Guidance, Control, and Dynamics*, Vol. 26, No. 5, pp. 728–733, 2003.

[10] D. McKinley, "Development of a Nonlinear Probability of Collision Tool for the Earth Observing System," *AIAA/AAS Astrodynamics Specialist Conference*, Keystone, Colorado, Paper 2006-6295, Aug. 2006.

[11] K. Chan, "Formulation of Collision Probability with Time-Dependent Probability Distribution Functions," *AAS/AIAA Space Flight Mechanics Meeting*, Williamsburg, VA, Paper 15-233, Jan. 2015.

[12] K.J. DeMars, Y. Cheng, and M.K. Jah, "Collision Probability with Gaussian Mixture Orbit Uncertainty," *Journal of Guidance, Control, and Dynamics*, Vol. 37, No. 3, pp. 979–985, 2014.

[13] R.W. Ghrist and D. Plakalovic, "Impact of Non-Gaussian Error Volumes on Conjunction Assessment Risk Analysis," *AIAA/AAS Astrodynamics Specialist Conference*, Minneapolis, Minnesota, Paper 2012-4965, Aug. 2012.

[14] J. T. Horwood, N. D. Aragon, and A. B. Poore, "Gaussian Sum Filters for Space Surveillance: Theory and Simulations," *Journal of Guidance, Control, and Dynamics*, Vol. 34, No. 6, pp. 1839–1851, 2011.

[15] V. Vittaldev and R.P. Russell, "Collision Probability for Space Objects Using Gaussian Mixture Models," *AAS/AIAA Space Flight Mechanics Meeting*, Kauai, HI, Paper 13-351, Feb. 2013.

[16] B.L. Livergood, "Implementation of 2014 Screening Volume Analysis," *Flight Dynamics Task Order 21 Technical Memorandum*, FDSS-21-0012, June 2014.

[17] S.W. Shepperd, "Universal Keplerian State Tranisition Matrix," *Celestial Mechanics*, Vol. 35, pp. 129-144, 1985.

[18] V.I. Lebedev and D.N. Laikov, "A Quadrature Formula for the Sphere of the 131st Algebraic Order of Accuracy," *Doklady Mathmatics*, Vol. 59, No. 3, pp 477-481, 1999.

[19] C. Sabol, et al., "Linearized Orbit Covariance Generation and Propagation Analysis via Simple Monte Carlo Simulations," *AAS/AIAA Space Flight Mechanics Meeting*, San Diego, CA, Paper 10-134, Feb. 2010.

[20] J.T. Horwood, N. Singh, J.M. Aristoff, A. Bhopale, "KRATOS: Kollision Risk Assessment Tool in Orbital Element Spaces," *The 2017 AMOS Conference*, Kihei HI, Sep 2016.